

Investigating recent deformation along the southern San Pedro Basin fault to assess evidence for connectivity between the San Pedro Basin and San Diego Trough fault systems

Principal Investigators: Jayne Bormann^{1*} and Graham Kent²

¹ Department of Geological Sciences
California State University, Long Beach
1250 Bellflower Blvd.
Long Beach, CA 90840
Phone: (562) 985-4975
Fax: (775) 784-4165
E-mail: jayne.bormann@csulb.edu

² Nevada Seismological Laboratory
University of Nevada, Reno MS174
1664 N. Virginia St.
Reno, NV 89557
Phone: (775) 784-4975
Fax: (775) 784-4165
E-mail: gkent@unr.edu

*now at the Nevada, Seismological Laboratory, University of Nevada, Reno. Email: jbormann@unr.edu

Term covered by the award: 9/1/2017-8/30/2018

Acknowledgement of Support and Disclaimer

This material is based upon work supported by the U.S. Geological Survey under Grant No. G17AP00124. The views and conclusions contained in this document are those of the authors and should not be interpreted as representing the opinions or policies of the U.S. Geological Survey. Mention of trade names or commercial products does not constitute their endorsement by the U.S. Geological Survey.

Abstract:

To address questions regarding the potential for throughgoing rupture between the San Diego Trough and San Pedro Basin faults, we collected 365 line-km of high-resolution multichannel seismic (MCS) reflection data along the southern San Pedro Basin fault between Avalon Knoll and Redondo Knoll. We acquired the data using California State University-Long Beach's 16-channel digital Geo-Eel hydrophone streamer with 6.25 m group spacing and a 2-kJ three-tip sparker energy source, resulting in 36 MCS reflection profiles with 3-5 m vertical resolution. We interpret the recency and style of deformation on the fault from the seismic profiles using the principles of sequence stratigraphy. The southern San Pedro Basin fault clearly offsets the seafloor on the margins of Avalon Knoll and Redondo Knoll at the southern and northern ends of the San Pedro Basin; however, the central portion of the fault is buried beneath 75-90 m of undeformed sediment (100-120 ms TWT thickness in seismic profile). Published vertical sediment accretion rates for the San Pedro Basin indicate that the marker horizon beneath the undeformed package has an age of 53-225 ka, with a poorly constrained preferred age of 225 ka. This suggests that although there are no apparent structural complexities that would inhibit throughgoing rupture between the San Diego Trough and San Pedro Basin fault systems, there is no evidence of Holocene slip on the southern San Pedro Basin fault in MCS reflection profiles. An alternate interpretation allows that the southern San Pedro Basin fault may have recent slip, but that right-lateral strike-slip displacement of horizontal sediments above the 53-225 ka marker horizon on the near vertical fault has resulted in offsets that are less than the 3-5 m vertical resolution of the MCS data.

1. Introduction

Geodetic measurements show that the San Andreas fault and other fault systems onshore in Southern California accommodate ~85% of the 50 mm/yr total Pacific/North American relative right-lateral plate motion, leaving offshore faults in the Inner California Borderlands (ICB) to accommodate the remaining 15% of plate boundary deformation (e.g., *Bennett et al.*, 1996; *Dixon et al.*, 2000; *Meade and Hagar*, 2005; *Platt and Becker*, 2010; *Hammond*, 2014). Between the Southern California coast and San Clemente Island, 6–8 mm/yr of right lateral shear strain accumulates across a ~100 km-wide zone that spans the Newport-Inglewood/Rose Canyon, Coronado Bank, Palos Verdes, San Diego Trough, and San Clemente fault systems (Figure 1). These offshore northwest-striking, sub-parallel, strike-slip faults work together to release the accumulated shear strain (*Grant and Rockwell*, 2002), posing significant yet poorly understood seismic hazard for Southern California’s densely populated coastal regions.

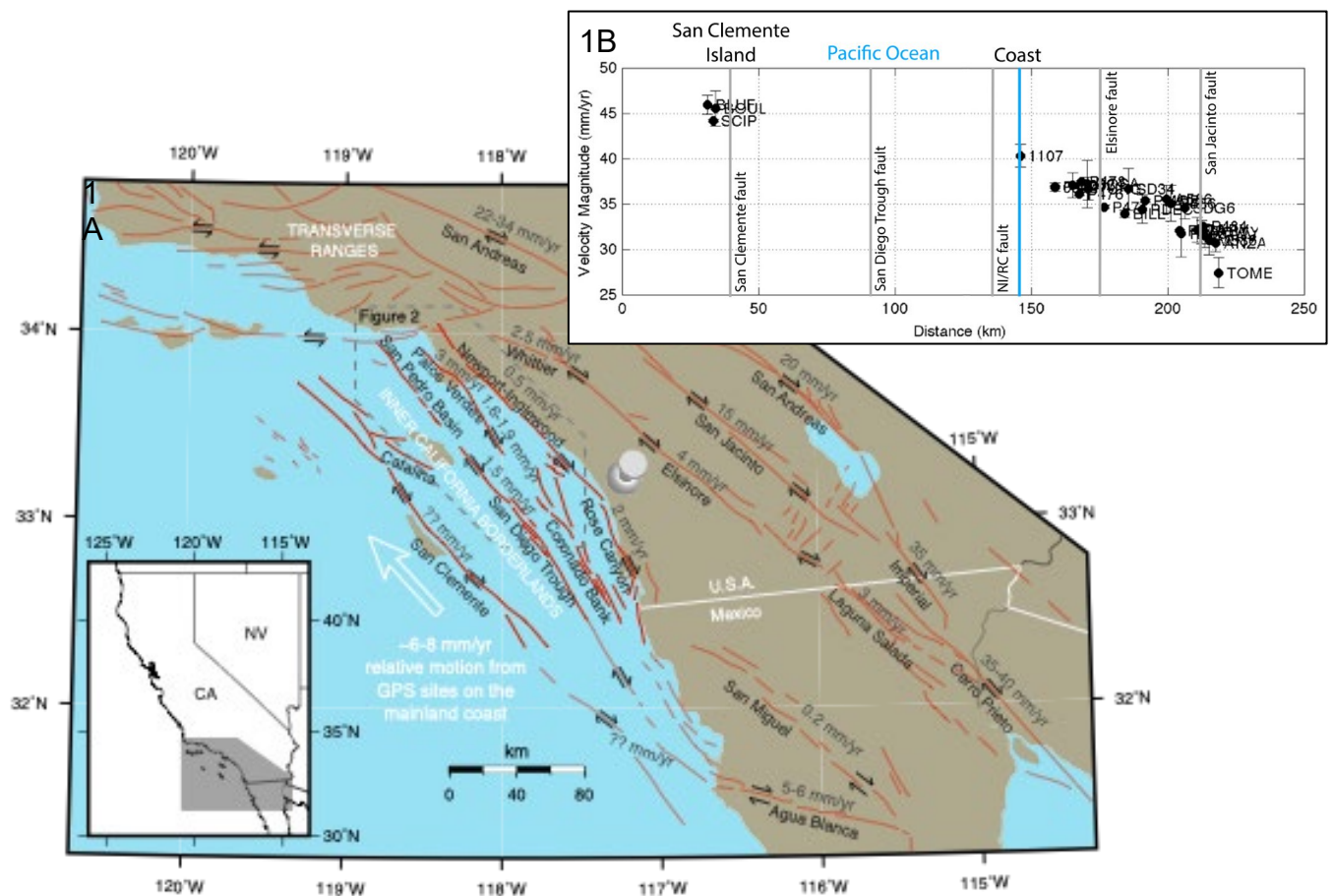


Figure 1. (A) Generalized fault map of Southern California with associated slip rate estimates. Major Southern California faults are shown in red lines, with traces of Inner California Borderland faults delineated by bold lines. Reported slip rates are the UCERF3 best rate estimates (Dawson et al., 2013), with the exception of the offshore Palos Verdes fault slip rate (Brothers et al., 2015). The gray dashed box marks the location of Figure 2. Inset map shows the location of the Inner California Borderlands in relation to the California and Mexico coastline. Figure and fault geometry modified from Rockwell et al., (2010) and Singleton et al., (2019). **(B)** Profile showing the magnitude of GPS velocities with respect to stable North America (NA12 reference frame) for sites spanning the ICB and southern California. Location of profile is shown by yellow box in Figure 1A. Velocities from *Hammond* (2014).

Recent work by *Ryan et al.* (2012) highlights the importance of the San Diego Trough fault in accommodating offshore deformation. They measure an offset wall of the San Gabriel Canyon to estimate a Holocene right-lateral slip rate of 1.5 ± 0.3 mm/yr, a rate that accounts for ~25% of the Inner California Borderlands deformation budget (see Figure 2 for slip-rate measurement location). Although *Ryan et al.* (2012) and *Francis and Legg* (2010) suggest that the San Diego Trough fault and the San Pedro basin fault may be one through-going fault system based on the orientation and location of the mapped fault traces, both studies lack high-resolution geophysical data in the San Pedro Basin to demonstrate this connection. The northernmost line in a 2013 high-resolution multichannel seismic reflection survey (*Driscoll et al.*, 2015a and 2015b) was the first profile to image the San Diego Trough fault offsetting the seafloor in the southern San Pedro Basin (*Bormann et al.*, in revision; profile shown in Figure 4D). This observation reduced the separation between the mapped traces of the two fault systems from ~10 km to <5 km, which is within the 5-km critical stepover distance where earthquake ruptures many propagate onto adjacent fault segments (e.g., *Wesnousky*, 2008). Linkage between the San Pedro Basin fault and the San Diego Trough/Bahia Soledad fault system increases the potential length of ruptures on the San Pedro Basin fault from 68 km to >330 km. Empirical magnitude-length scaling relationships indicate that an end-to-end rupture of the combined fault system could produce a M_w 7.7-7.9 earthquake, posing significant and unevaluated hazard for communities and coastal infrastructure in the Los Angeles metropolitan area.

This study maps the geometry of the southern San Pedro Basin fault using newly collected high-resolution multichannel seismic reflection profiles from the San Pedro Basin and constrains the relative recency of deformation along the fault using the principles of sequence stratigraphy. Our survey infills a 25-km gap between previously existing high-resolution seismic reflection datasets covering the northern San Pedro Basin fault in the Santa Monica Basin (yellow grid, Figure 2), and the San Diego Trough fault in the Gulf of Santa Catalina to the south (red grid, Figure 2). We combine the new constraints with prior results from the San Diego Trough fault (*Bormann et al.*, in revision; *Ryan et al.*, 2012) to evaluate the potential for connectivity between the two faults. Understanding the recency of deformation allows us to evaluate the structural and temporal relationships between the San Diego Trough and San Pedro Basin faults, which, in turn, helps constrain the potential rupture length and maximum expected magnitude for future earthquakes on both faults.

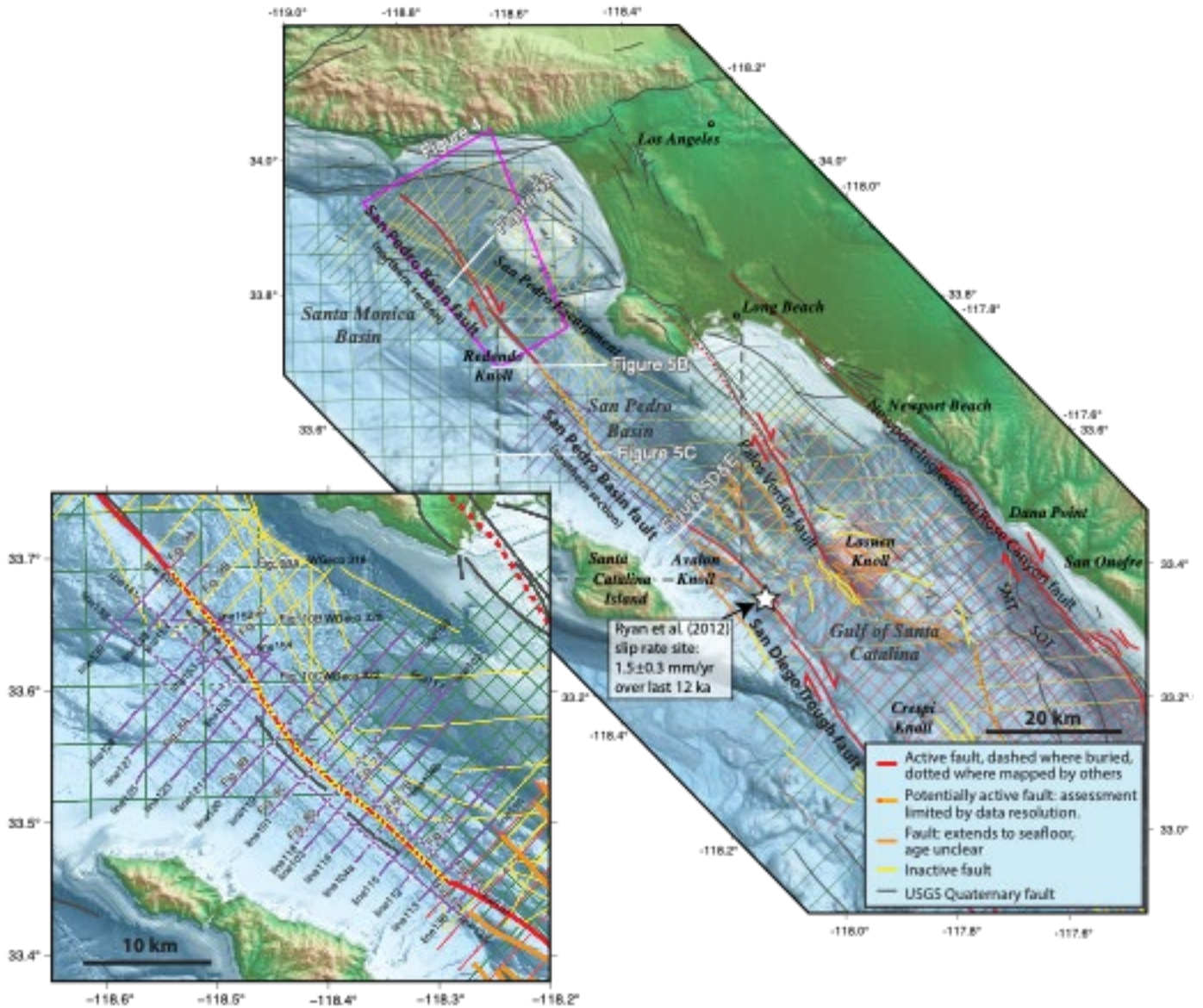


Figure 2. San Pedro Basin fault map and southern San Pedro Basin fault survey map (inset). Purple grid shows the location of R/V Yellowfin MCS profiles collected during this project. Dashed box marks the extent of the southern San Pedro Basin fault inset map. Magenta polygon denotes extent of the 3D perspective view of the northern San Pedro Basin fault shown in Figure 4. White lines mark the locations of seismic profiles displayed in Figure 5. Fault locations and age of deformation interpreted from data collected during this project (purple grid) and previous regional seismic surveys: SIO/UNR regional high-resolution 2D MCS dataset (red grid, *Driscoll et al.*, 2015a and 2015b), high-resolution MCS data acquired by the USGS between 1998-2001 (yellow grid, Normark et al., 1999a and 1999b; Sliter et al., 2005), deep-penetration MCS surveys collected by WesternGeco (W-30-81-SC and W-5-82-SC) archived at the National Archive of Marine Seismic Surveys (<http://walrus.wr.usgs.gov/namss/>); and 25-m multibeam bathymetry (Dartnell et al., 2015). Fault map modified from *Bormann et al.* (in revision). Mapping of the Newport- Inglewood/Rose Canyon fault from Sahakian et al. (2014). Abbreviations: San Mateo Trend (SMT) and San Onofre Trend (SOT).

2. Seismic Data

Our approach for this project was to acquire high-resolution multichannel seismic reflection profiles using California State University, Long Beach's marine geophysical equipment aboard the R/V Yellowfin during the spring and summer of 2018. The Southern California Marine Institute operates the R/V Yellowfin out of Terminal Island in Los Angeles Harbor. The science party consisted of PIs Bormann (CSULB) and Kent (UNR), and graduate students from California State University, Long Beach and the Scripps Institution of Oceanography. The survey was conducted in a series of one-day cruises between Los Angeles Harbor and Two Harbors on Catalina Island during April-June 2018. In total, the survey consisted of 10 days of marine seismic reflection data acquisition. We collected 33 new profiles totaling 365 line-km of high-resolution multichannel seismic reflection data (Table 1, Figure 2 – purple grid). We acquired the data using California State University-Long Beach's 16-channel digital Geo-Eel hydrophone streamer with 6.25 m group spacing and a 2-kJ three-tip sparker energy source. We towed both the source and the streamer at 3 m depth, with a near offset of 25 m. The survey speed ranged between 4.0-5.0 knots in favorable weather conditions with swells of less than 2 m. The shot interval was 3 seconds, resulting in a nominal common mid-point spacing of 3.125 m. The reflected waveforms were sampled at 0.5 ms intervals for 2.5 seconds to image roughly twice the maximum seafloor depth.

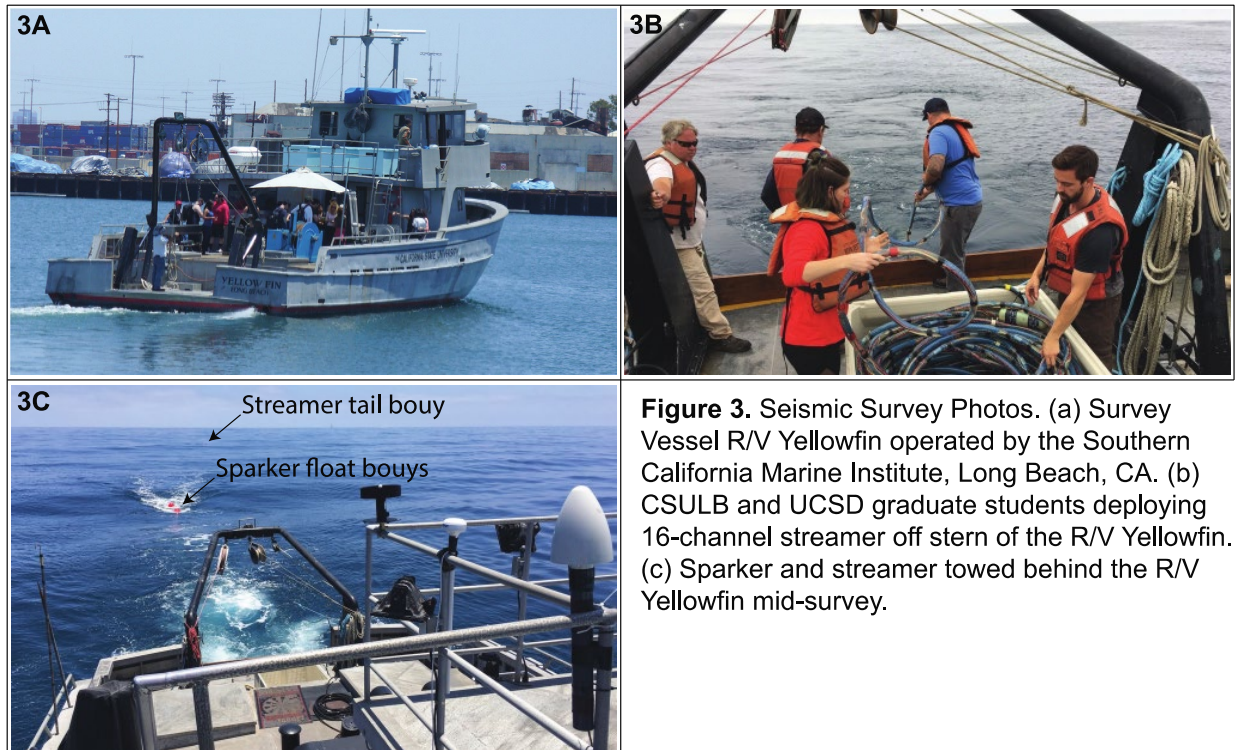


Figure 3. Seismic Survey Photos. (a) Survey Vessel R/V Yellowfin operated by the Southern California Marine Institute, Long Beach, CA. (b) CSULB and UCSD graduate students deploying 16-channel streamer off stern of the R/V Yellowfin. (c) Sparker and streamer towed behind the R/V Yellowfin mid-survey.

We processed the data using a combination of Matlab and Sioseis (Henkart, 2003). The processing workflow consisted of (1) assigning source and receiver geometry to the shot records, (2) trace editing, (3) sorting the shot gathers to create CMP gathers, (4) minimum-phase bandpass filtering (5) applying a normal moveout correction, (6) stacking the CMP gathers into single CMP traces, and (7) frequency-wave number (f-k) migration. All processing and travel-time to depth conversions in this paper assume water column and sediment velocities of 1500 m/s. The processed data contain acoustic frequencies between 50-200 Hz, resulting in

a vertical resolution of ~3-5 m with maximum penetration over 1000 ms (~750 m) beneath the seafloor.

The nominal fault-perpendicular line spacing of the newly acquired grid is 2.0 km, and it extends between Redondo Knoll in the northwest and Avalon Knoll in the southeast (Figure 2, purple grid). We supplement this dataset with high-resolution MCS profiles collected by the USGS (*Normark et al.*, 1999a; *Normark et al.*, 1999b; *Sliter et al.*, 2005; data available at <http://cmgds.marine.usgs.gov/>) and the Scripps Institution of Oceanography and the University of Nevada, Reno (*Driscoll et al.*, 2015a and 2015b); deep-penetration legacy industry MCS profiles collected by WesternGeco in 1981 and 1982 (surveys W-30-81-SC and W-5-82-SC, respectively) that are archived in the National Archive of Marine Seismic Surveys (NAMSS) (*Triezenberg et al.*, 2016; data available at <http://walrus.wr.usgs.gov/NAMSS/>); and a 25-m resolution regional multibeam bathymetry digital elevation model (*Dartnell et al.*, 2015). The USGS Coastal and Marine Geoscience Data System (CMGDS) and NAMSS archives provide the original shot point locations for the USGS and industry surveys, however data gaps and mismatches between the shot locations and seismic traces exist for many profiles. We used the original shot point locations and survey configurations to calculate CMP locations for each survey and performed quality control on the datasets to account for gaps in the seismic records and ensure correlation between the seafloor in our relocated seismic profiles and multibeam bathymetry.

Table 1. San Pedro Basin MCS survey track information.

Line Name	Line Start		Line End		Ship Heading	Track Azimuth (°)	Track Distance (km)	Date Acquired
	lat (°)	lon (°)	lat (°)	lon (°)				
Line 100	33.63063	-118.31637	33.61358	-118.33433	SW	221	2.52	2018-04-28
Line 101	33.61190	-118.33614	33.50339	-118.45453	SW	222	16.33	2018-04-28
Line 102	33.60601	-118.28797	33.53233	-118.36647	SW	222	10.97	2018-04-29
Line 103	33.53424	-118.36501	33.47806	-118.42331	SW	221	8.27	2018-04-29
Line 104a	33.46827	-118.37680	33.47636	-118.36951	NE	37	1.13	2018-04-29
Line 104b	33.47732	-118.36864	33.52032	-118.32810	NE	38	6.09	2018-06-14
Line 112	33.54666	-118.23661	33.45014	-118.33613	SW	221	14.17	2018-06-14
Line 113	33.43908	-118.32003	33.50234	-118.25063	NE	42	9.55	2018-06-14
Line 114	33.50841	-118.25025	33.52587	-118.27668	NW	308	3.13	2018-06-14
Line 115	33.51956	-118.29145	33.45908	-118.35617	SW	222	9.02	2018-06-14
Line 116	33.47587	-118.39926	33.58375	-118.28299	NE	42	16.14	2018-06-15
Line 117	33.59564	-118.29751	33.60155	-118.31516	WNW	292	1.76	2018-06-15
Line 118	33.60120	-118.32147	33.48273	-118.43025	SW	217	16.61	2018-06-15
Line 119	33.51970	-118.46664	33.64615	-118.33034	NE	42	18.92	2018-06-15
Line 120	33.64842	-118.35579	33.51701	-118.49781	SW	222	19.68	2018-06-18
Line 121	33.53039	-118.51400	33.60652	-118.43133	NE	42	11.43	2018-06-18
Line 123	33.61990	-118.44793	33.52985	-118.54388	SW	222	13.41	2018-06-18
Line 125	33.52820	-118.57425	33.64058	-118.45575	NE	41	16.65	2018-06-19
Line 127	33.63777	-118.48606	33.54975	-118.57929	SW	221	13.07	2018-06-19
Line 128	33.56376	-118.59353	33.65500	-118.49401	NE	42	13.72	2018-06-19
Line 130	33.70135	-118.53098	33.63450	-118.60427	SW	222	10.07	2018-06-26
Line 132	33.65415	-118.60071	33.49237	-118.37372	SE	130	27.70	2018-06-26
Line 135	33.50749	-118.39477	33.42854	-118.28248	SE	130	13.64	2018-06-27
Line 136	33.43015	-118.29387	33.45537	-118.26585	NE	43	3.83	2018-06-27
Line 137	33.44645	-118.26515	33.58929	-118.46395	NW	311	24.36	2018-06-27
Line 141	33.56555	-118.43295	33.66999	-118.57406	NW	312	17.50	2018-06-28

Line 143	33.64352	-118.56362	33.69365	-118.50983	NE	42	7.48	2018-06-28
Line 145	33.67996	-118.53885	33.58464	-118.40649	SE	131	16.22	2018-06-28
Line 151	33.67238	-118.52131	33.65043	-118.54364	SW	220	3.20	2018-06-29
Line 152	33.65174	-118.54264	33.64958	-118.48724	E	93	5.14	2018-06-29
Line 153	33.64807	-118.48678	33.62073	-118.51982	SW	225	4.32	2018-06-29
Line 154	33.61908	-118.51805	33.62715	-118.45389	E	81	6.01	2018-06-29
Line 155	33.62587	-118.45373	33.59401	-118.49012	SW	224	4.89	2018-06-29

3. Previous Fault Mapping

The northern San Pedro Basin fault has robust seafloor strike-slip geomorphic expression as the fault cuts through the Santa Monica Basin. The fault clearly offsets the seafloor in both multibeam bathymetry (Figure 4) and high-resolution seismic reflection profiles (Figure 5A and B), demonstrating alternating uphill and downhill facing linear scarps, pressure ridges, and a steeply dipping fault trace. Recent activity on this portion of the fault is well documented by Fisher *et al.* (2003), Bohannon *et al.*, (2004), and Paull *et al.* (2008).

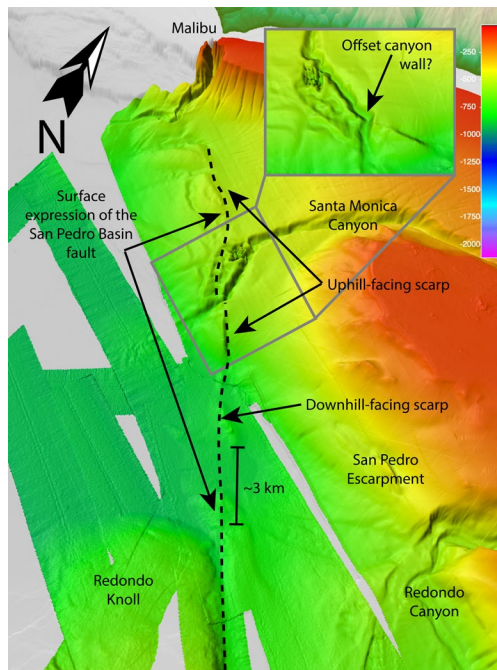


Figure 4. 3D perspective view of the San Pedro Basin fault offsetting marine sediments in the Santa Monica Basin. The fault exhibits classic strike-slip fault geomorphic features including alternate facing scarps and pressure ridges. Inset shows a possible right-lateral offset of the Santa Monica Canyon wall. Scene location shown by magenta box in Figure 2.

Less is known about the southern San Pedro Basin fault due to a lack of high-resolution geophysical data in the San Pedro Basin. Although many maps and fault models identify this section as active (e.g., Junger and Wagner, 1977; Fisher *et al.*, 2003; Bohannon *et al.*, 2004; Legg *et al.*, 2007, 2015; Plesch *et al.*, 2007; Paull *et al.*, 2008; Francis and Legg, 2010; Sorlien *et al.*, 2013), none of these publications image the fault offsetting the seafloor or young sedimentary packages in the San Pedro Basin. Previous mapping of the southern San Pedro Basin fault is based on legacy seismic reflection datasets collected during the early 1980's that image the fault offsetting stratigraphy at depth (Figure 5C). Using only the previously existing datasets, a 30-km gap exists between observations of seafloor offset by the San Pedro Basin fault, southeast of Redondo Knoll, and seafloor offset by the San Diego Trough fault, north of Avalon Knoll (Figure 2). These observations make it unclear if the southern San Pedro Basin fault is no longer active, or alternatively, if the vertical offsets that result from strike-slip motion on the fault are less than the 7-10 m vertical resolution of the legacy datasets (see Figure 5D and E for comparison of dataset resolution).

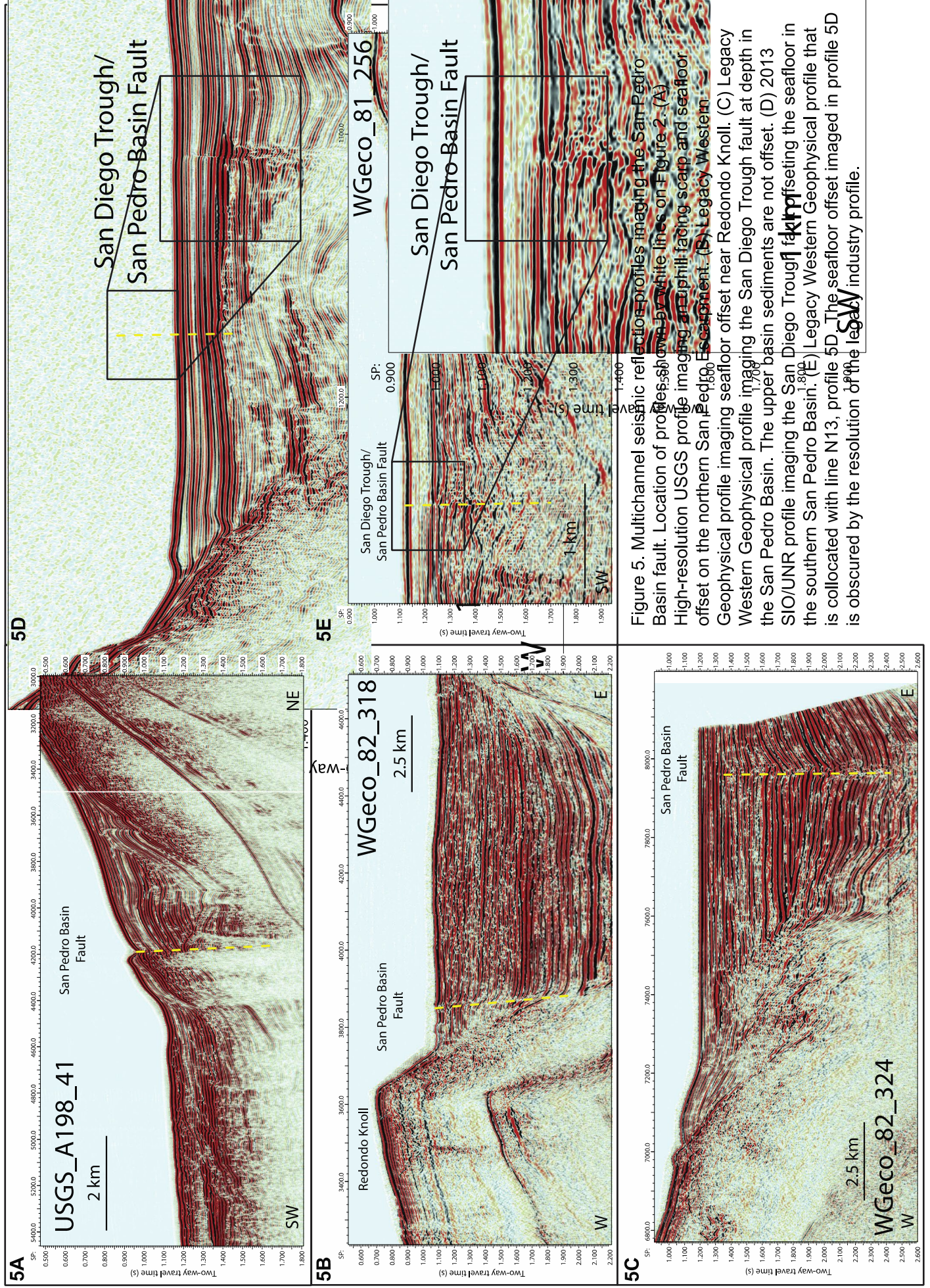


Figure 5. Multichannel seismic reflection profiles imaging the San Pedro Basin fault. Location of profiles shown by white lines on Figure 2. (A) High-resolution USGS profile imaging an uplift-facing scarp and seafloor offset on the northern San Pedro Escarpment. (B) Legacy Western Geophysical profile imaging seafloor offset near Redondo Knoll. (C) Legacy Western Geophysical profile imaging the San Diego Trough fault at depth in the San Pedro Basin. The upper basin sediments are not offset. (D) 2013 SIO/UNR profile imaging the San Diego Trough fault offsetting the seafloor in the southern San Pedro Basin. (E) Legacy Western Geophysical profile that is collocated with line N13, profile 5D. The seafloor offset imaged in profile 5D is obscured by the resolution of the legacy industry profile.

4. Results

Here we describe the key relationships between structure and subsurface stratigraphy imaged in the newly collected MCS data to constrain the recency of slip on the southern San Pedro Basin fault and the potential for throughgoing rupture on the San Diego Trough and San Pedro Basin faults. The age of sediment in the San Pedro Basin are poorly constrained. Accordingly, we interpret the recency of fault slip using sequence stratigraphic interpretation techniques (*Christie-Blick and Driscoll, 1995*) and the thickness of sediment that overlies the fault. We identify two marker horizons (e.g., Figure 6) that extend throughout the basin and use these horizons to constrain the relative timing of deformation.

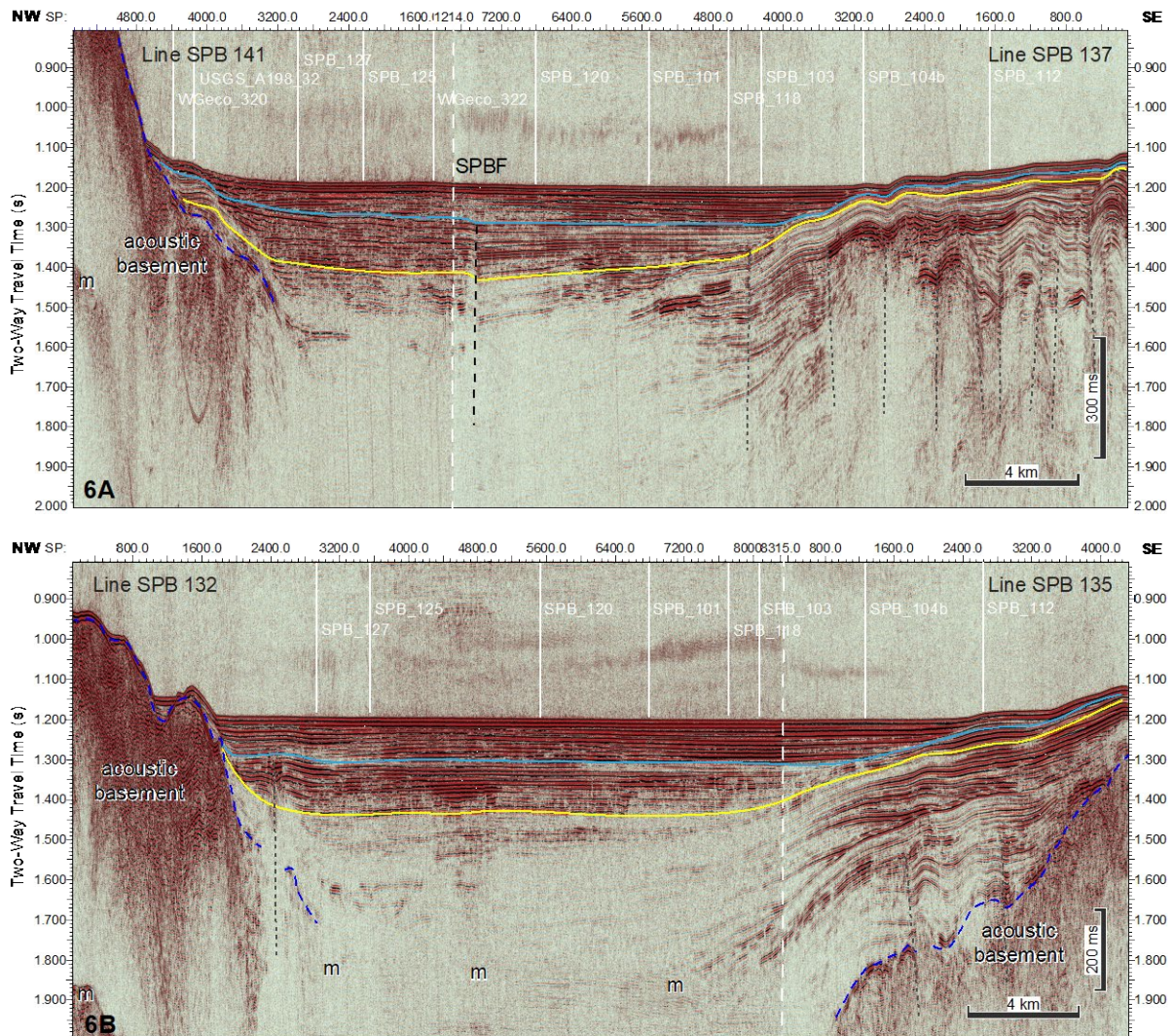


Figure 6. Seismic reflection profiles that span the San Pedro Basin. See Figure 2 for profile locations. Thicker black dashed line marks the location of the San Pedro Basin fault. Thinner gray dashed lines mark the location of other faults that appear to be inactive. Yellow and blue horizons are marker horizons that are used consistently throughout the report. Labeled white lines above the seafloor mark the intersections with fault perpendicular profiles shown Figures 7-10, and the dashed white lines mark the location of the seam between the two seismic lines shown in each profile.

Stratigraphy

Figure 6 shows two fault parallel seismic profiles that span the length of the San Pedro Basin between Redondo Knoll in the northwest to Avalon Knoll in the southeast. Both profiles show similar stratigraphic relationships where folded and acoustically transparent deeper sedimentary packages are onlapped by younger, relatively flat-lying, high-amplitude strata. This unconformity is denoted with a yellow marker horizon (SPB-20) we trace throughout the basin. We identify an upper blue marker horizon (SPB-10) within the high-amplitude package that caps deformation associated with the San Pedro Basin fault in the San Pedro Basin. The blue and yellow marker horizons are shallowest in the southeast, within 20 ms and 40 ms Two-Way Travel Time (TWTT) of the seafloor, respectively, as the fault-parallel profiles approach the Avalon Knoll basement high. The blue and yellow marker horizons are deepest in the center of the basin at 100 ms and 220 ms TWTT beneath the seafloor, shallowing as they onlap basement at Redondo Knoll.

Structure

Figure 5D shows a structure that is continuous with the San Diego Trough fault offsetting the seafloor with an apparent down to the northeast displacement in high-resolution MCS data (*Driscoll et al.*, 2015b) along the northwestern margin of Avalon Knoll in the San Pedro Basin. *Bormann et al.* (in revision) interpret this profile as evidence that the San Diego Trough fault and the San Pedro Basin fault may be one continuous structure. Figure 7 images this structure as it continues north. Profiles SPB_112, SPB_104b, and SPB_103 (Figures 7C, 7B, and 7A) image the top of this structure buried by an increasing thickness of sediment as the fault extends north into the San Pedro Basin. The sense of apparent offset changes polarity from down to the northeast in profile SPB_112 to down to the southwest in profiles SPB_104b and SPB_103.

Continuing north, Figure 8 images the fault as it cuts sediments in the central San Pedro Basin. In this section, the upper limit of offset imaged on the San Pedro Basin fault is buried by 100-150 ms TWTT of undeformed sediment, and all strata above the blue marker horizon remain undeformed. The fault once again changes polarity, with the apparent offset changing from down to the southwest in profiles SPB_118 and SPB_101 (Figure 8D and 8C) to down to the northeast in profiles SPB_120 and SPB_125 (Figures 8B and 8A). The fault intersects profile SPB_137 (Figure 6A) between profiles SPB_120 and SPB_125, with an apparent down to the southeast displacement, suggesting that the true displacement in this section of the fault is likely down to the east.

Continuing north, Figure 8 images the fault as it cuts sediments in the central San Pedro Basin. In this section, the upper limit of offset imaged on the San Pedro Basin fault is buried by 100-150 ms TWTT of undeformed sediment, and all strata above the blue marker horizon remain undeformed. The fault once again changes polarity, with the apparent offset changing from down to the southwest in profiles SPB_118 and SPB_101 (Figure 8D and 8C) to down to the northeast in profiles SPB_120 and SPB_125 (Figures 8B and 8A). The fault intersects profile SPB_137 (Figure 6A) between profiles SPB_120 and SPB_125, with an apparent down to the southeast displacement, suggesting that the true displacement in this section of the fault is likely down to the east.

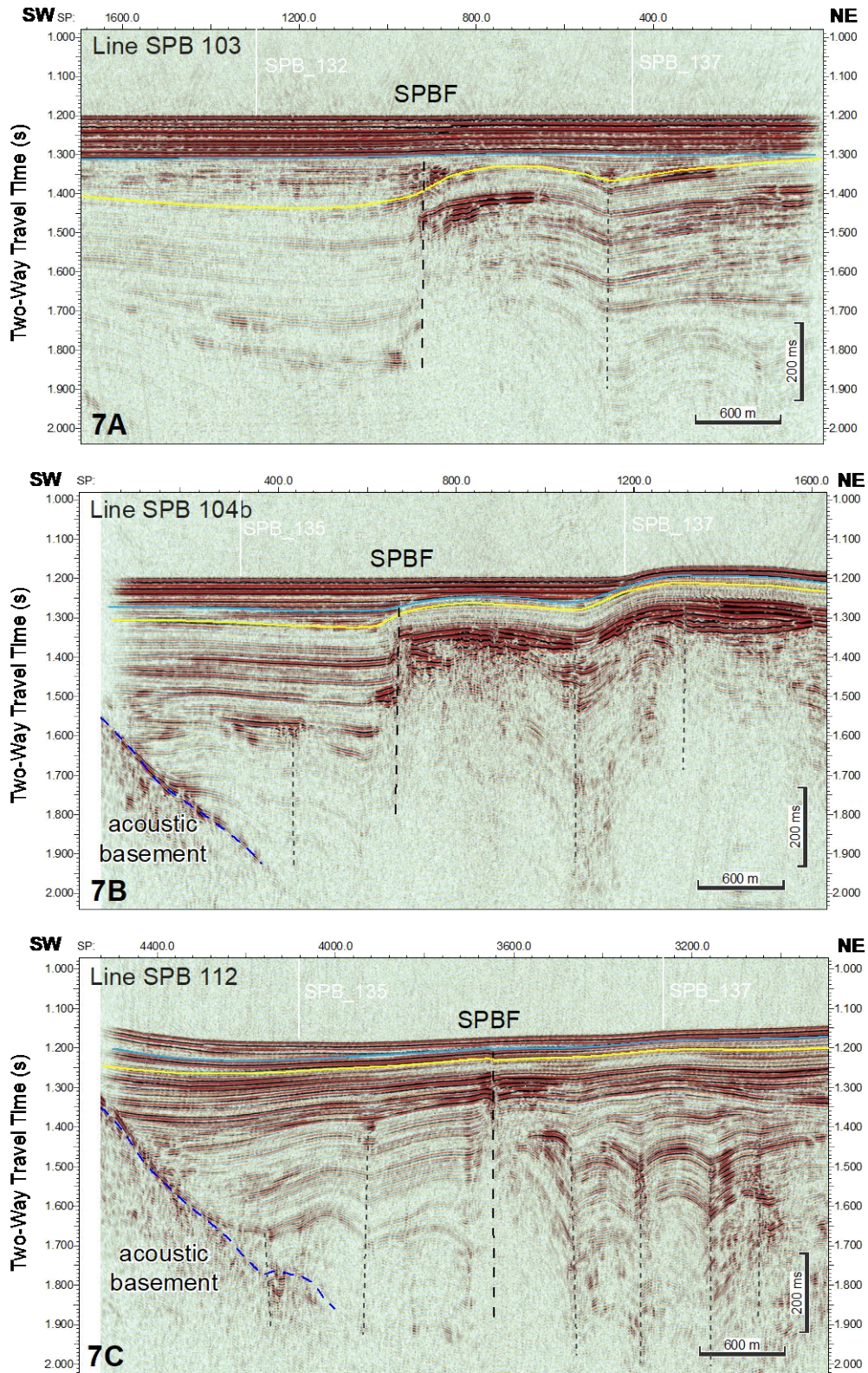


Figure 7. Seismic reflection profiles across the southern San Pedro Basin fault in the southern San Pedro Basin. See Figure 2 for profile locations. Thicker black dashed line marks the location of the San Pedro Basin fault. Thinner gray dashed lines mark the location of other faults that appear to be inactive. Yellow and blue horizons are marker horizons that are used consistently throughout the report. Labeled white lines above the seafloor mark intersections with fault parallel profiles shown in Figure 6.

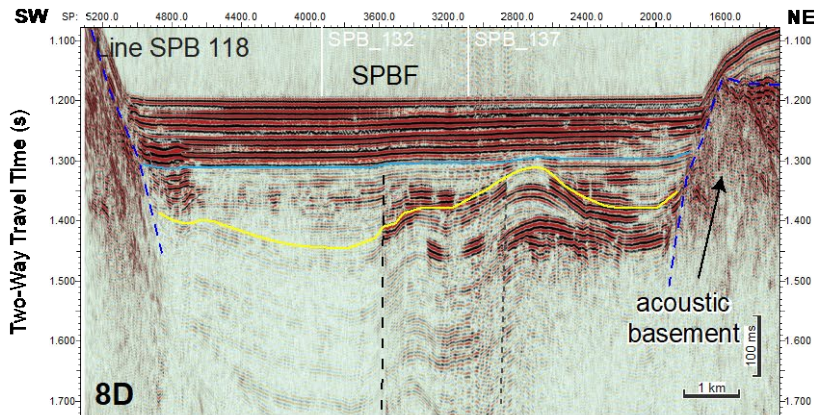
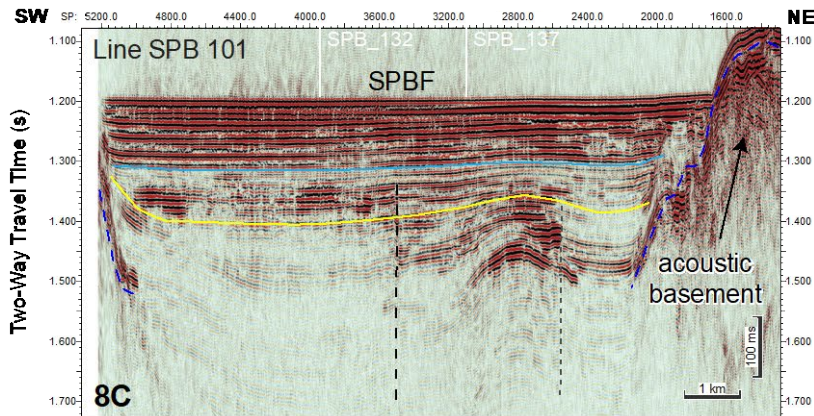
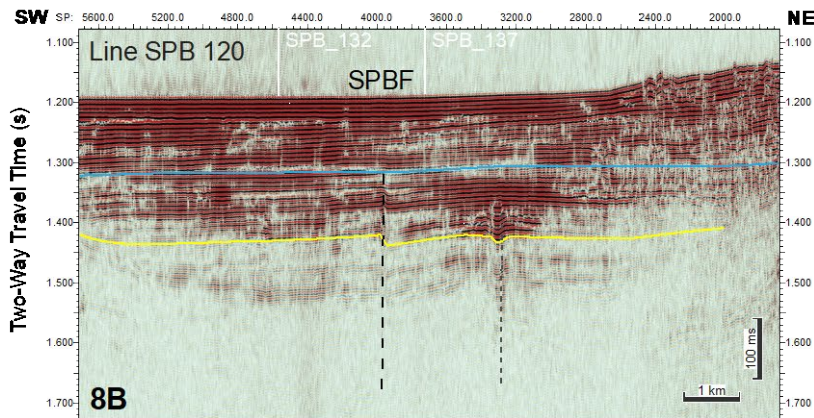
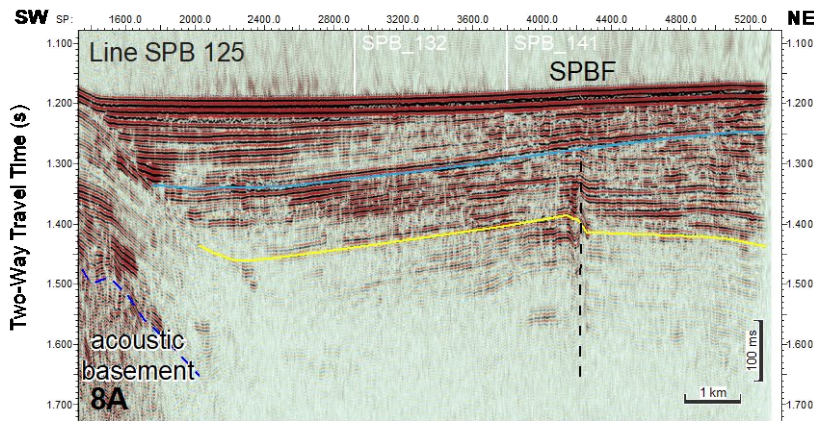


Figure 8. Seismic reflection profiles across the southern San Pedro Basin fault in the central San Pedro Basin. See Figure 2 for profile locations. Thicker black dashed line marks the location of the San Pedro Basin fault. Thinner gray dashed lines mark the location of other faults that appear to be inactive. Yellow and blue horizons are marker horizons that are used consistently throughout the report. Labeled white lines above the seafloor mark the intersections with fault parallel profiles shown in Figure 6.

North of profile SPB_125, the sedimentary package overlying the blue marker horizon thins (Figure 9). Deformation on the San Pedro Basin fault remains beneath the blue horizon (Figures 9B and 9C), until profile SPB_130 (Figure 9A), where the fault clearly offsets young Redondo Canyon fan deposits at the surface along the eastern margin of Redondo Knoll. The relative vertical displacement along the upper extent of the fault in the northern San Pedro Basin is relatively small, and in some profiles, it is difficult to confidently identify the fault. Our fault northern San Pedro Basin fault locations correspond with those imaged in deep-penetrating legacy WesternGeco profiles (Figure 10).

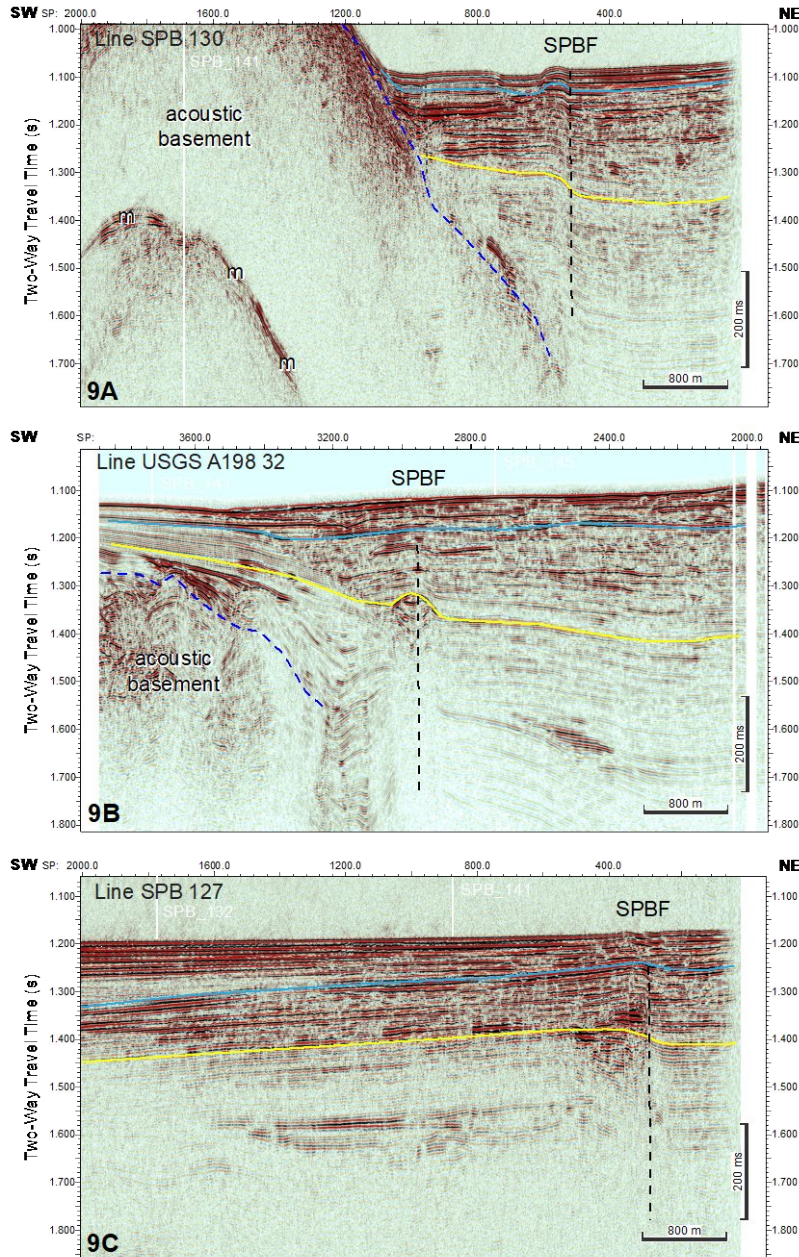


Figure 9. Seismic reflection profiles across the southern San Pedro Basin fault in the northern San Pedro Basin. See Figure 2 for profile locations. Thicker black dashed line marks the location of the San Pedro Basin fault. Thinner gray dashed lines mark the location of other faults that appear to be inactive. Yellow and blue horizons are marker horizons that are used consistently throughout the report. Labeled white lines above the seafloor mark the intersections with fault parallel profiles shown in Figure 6.

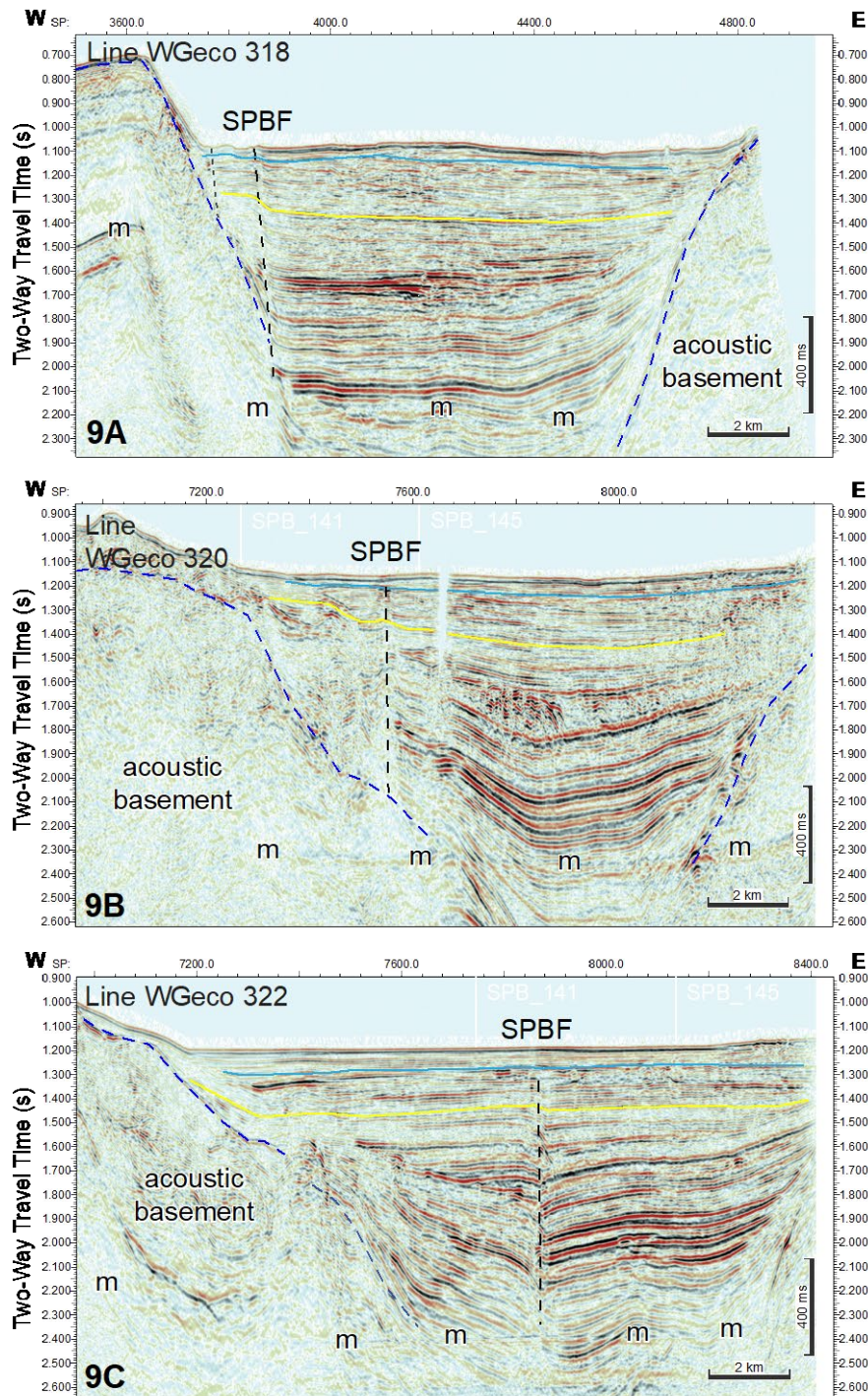


Figure 10. WesternGeco legacy deep-penetration seismic reflection profiles across the southern San Pedro Basin fault in the northern San Pedro Basin. See Figure 2 for profile locations. Thicker black dashed line marks the location of the San Pedro Basin fault. Thinner gray dashed lines mark the location of other faults that appear to be inactive. Yellow and blue horizons are marker horizons that are used consistently throughout the report. Labeled white lines above the seafloor mark the intersections with fault parallel profiles shown in Figure 6.

Recency of faulting and fault system connectivity

The southern San Pedro Basin fault only cuts seafloor sediments in the northern and southern ends of the basin near Redondo and Avalon Knoll respectively. These fault exposures are separated by a distance of 25-30 km. For much of this distance, the uppermost deformation associated with the fault is buried beneath between 100-120 ms TWTT of sediment. Assuming a shallow sediment velocity of 1500 m/s results in a sedimentary thickness for the package that overlies the blue marker horizon of 75-90 m. Sediment vertical accretion rates for the San Pedro Basin are poorly constrained, highly variable, and range between 40-100 cm/ka (Table 2). Applying these sedimentation rates to estimate the age of the blue marker horizon of results in

age estimates between 53-225 ka. We consider these constraints to be highly speculative, and we favor the vertical accretion rates determined from 510P2 piston core due to the longer length of sediment recovered. This results in a preferred age for the blue marker horizon of 225 ka.

Although uncertain, the 225 ka age for the blue marker horizon indicates that the southern San Pedro Basin fault has not accumulated significant vertical offset during the Holocene. Both the northern San Pedro Basin fault to the north and the San Diego Trough fault to the south exhibit robust seafloor geomorphic expression in Holocene sediment. This indicates that although subsurface traces of the faults are continuous and there are no readily apparent structural complexities to inhibit through-going rupture, the high-resolution MCS data collected for this survey do not provide evidence for simultaneous rupture of the two fault systems. This is a tentative interpretation. An alternative interpretation may be that the recency of deformation on the southern San Pedro Basin fault is inconclusive. Motion along the San Pedro Basin fault is expected to be predominately right-lateral strike-slip, and the basin sediments above the blue marker horizon are nearly horizontal. Strike-slip motion along the southern San Pedro Basin fault is supported by the near vertical fault dip and the reversed sense of apparent offset along the trace of the fault. With these factors in mind, offset in the uppermost sediments may be smaller than the 3-5 m resolution of the sparker dataset collected for this survey.

Table 2. San Pedro Basin sediment vertical accretion rates

Cruise	Core	Water depth (m)	Core Length (m)	Core Type	Vertical Accretion Rate (cm/ka)	Reference
A103SC	SP1	-	<0.3	Piston	45.8*	<i>Normark et al., 2009</i>
O299SC	510P2	-	4.50	Piston	41.8*	<i>Normark et al., 2009</i>
A103SC	647	898	0.37	Box	70**	<i>Alexander and Lee, 2009</i>
A103SC	650	830	0.39	Box	140**	<i>Alexander and Lee, 2009</i>
A103SC	4444	855	0.39	Box	100**	<i>Alexander and Lee, 2009</i>
A103SC	4460	830	0.38	Box	100**	<i>Alexander and Lee, 2009</i>

* Rates for cores without base of the Holocene recovered

** Rates originally given in cm/yr

5. Broader Impacts and Dissemination

This project supported research costs and salary for an early career faculty member (PI Bormann). Six graduate students from California State University, Long Beach and Scripps Institution of Oceanography/University of California, San Diego gained hands-on experience deploying marine geophysical instrumentation and acquiring multichannel seismic reflection data. CSULB undergraduate students in Bormann's 2018 Introduction to Geophysics course also gained exposure to marine geophysics, seismic interpretation, and fault mapping by helping acquire data for the survey and subsequently interpreting these data in classroom exercises. Results from this work have been presented at the 2018 Seismological Society of America Meeting, the 2018 12th Joint Meeting of the United States-Japan Cooperative Program in Natural Resources (UJNR) panel on Earthquake Research in Kumamoto, Japan, and will be submitted for publication to the Bulletin of the Seismological Society of America of similar journal pending results of complimentary projects on the San Diego Trough fault.

Bormann, J.M., G.M. Kent, N.W. Driscoll, V.J. Sahakian, J.M. Maloney, and A.J. Harding, 2018, Characterizing hazard for low-slip-rate strike-slip faults offshore Southern

California, 12th Joint Meeting of the United States-Japan Natural Resources Panel of Earthquake Research, Kumamoto, Japan, October 24-26, 2018.

Bormann, J.M., C.J. Ruhl, G.M. Kent, N.W. Driscoll, and A.J. Harding, 2018, Hazards From the Sea: Rupture Scenarios for the San Diego Trough and San Pedro Basin fault systems, offshore Southern California, *Seismology of the Americas*, Miami, FL, May 14-17, *Seismological Research Letters*, v. 89(2B), p. 803.

6. Seismic Data Archival and Availability

Seismic data collected for this project are archived in the Harvard Dataverse in the San Pedro Basin fault marine seismic dataverse (https://dataverse.harvard.edu/dataverse/SPBF_seismic). Datasets housed within the dataverse, including raw and processed segy files, navigation data, line plots, and metadata are archived at the link below.

Bormann, Jayne, 2021, "2018 San Pedro Basin fault CSULB multichannel seismic reflection data", <https://doi.org/10.7910/DVN/EGB21M>, Harvard Dataverse, V1

7. Acknowledgements

Special thanks go to Captains Dennis Dunn and Joel Ingram, engineer Denis Mahaffy, and the crew of the R/V Yellowfin for their support in safely completing the seismic survey. We also thank geophysical engineers Mike Barth and Doug Bowlus generously sharing their knowledge in mobilizing and troubleshooting the marine geophysical equipment. We thank Dan Boyd (CSULB), Boe Derosier (UCSD), James Holmes (UCSD), Daniel Schwartz (UCSD), Amber Tucker (CSULB), Emily Wei (UCSD), and the CSULB 2018 Introduction to Geophysics students for assisting with mobilization, deployment, and acquisition for the seismic survey. Use of Kingdom seismic interpretation software was provided by generous grants from IHS Markit to California State University, Long Beach and the University of Nevada, Reno.

8. References

- Alexander, C.R., and Lee, H.J., 2009, Sediment accumulation on the Southern California Bight continental margin during the twentieth century, in Lee, H.J., and Normark, W.R., eds., *Earth Science in the Urban Ocean: The Southern California Continental Borderland: Geological Society of America Special Paper 454*, p. 69–87, doi: 10.1130/2009.2454(2.4).
- Bennett, R.A., Rodi, W., and Reilinger, R.E., 1996, Global Positioning System constraints on fault slip rates in southern California and northern Baja, Mexico: *Journal of Geophysical Research*, v. 101, no. B10, p. 21943–21960, doi: 10.1029/96JB02488.
- Bohannon, R.G., Gardner, J.V., and R.S. Sliter, 2004, Holocene to Pliocene tectonic evolution of the region offshore of the Los Angeles urban corridor, southern California: *Tectonics*, v. 23, TC1016, doi:10.1029/2003TC001504.
- Bormann, J.M., Kent, G.M., Driscoll, N.W., Harding, A.J., and Wesnousky, S.G., *in revision*, Active faulting in the Gulf of California and San Diego Trough, Inner California Borderland, offshore Southern California: for consideration in *Geosphere*.
- Brothers, D.S., Conrad, J.E., Maier, K.L., Paull, C.E., McGann, M., and Caress, D.W., 2015, The Palos Verdes Fault offshore Southern California: Late Pleistocene to present tectonic geomorphology, seascape evolution, and slip rate estimate based on AUV and ROV surveys: *Journal of Geophysical Research: Solid Earth* (1978–2012), v. 120, p. 4734–4758, doi: 10.1002/2015JB011938.

- Christie-Blick, N. and Driscoll, N.W., 1995, Sequence Stratigraphy: Annual Review of Earth and Planetary Science, v. 23, p. 451-478.
- Dixon, T., Farina, F., DeMets, C., Suarez-Vidal, F., Fletcher, J., Marquez-Azua, B., Miller, M., Sanchez, O., and Umhoefer, P., 2000, New Kinematic models for Pacific-North America motion from 3 Ma to present, II: Evidence for a "Baja California shear zone": Geophysical Research Letters, v. 27, no. 23, p. 3961–3964, doi: 10.1029/2000GL008529.
- Dartnell, P., Driscoll, N.W., Brothers, D., Conrad, J.E., Kluesner, J., Kent, G., and Andrews, B., 2015, Colored shaded-relief bathymetry, acoustic backscatter, and selected perspective views of the inner continental borderland, Southern California: U.S. Geological Survey Scientific Investigations Map 3324, 3 sheets, <http://dx.doi.org/10.3133/sim3324>.
- Driscoll, N., Kent, G., and Bormann, J., 2015a, Processed multi-channel seismic data (stacks and migrations) offshore California acquired during R/V Melville expedition MV1316 (2013): Academic Seismic Portal at UTIG, Marine Geoscience Data System, <http://dx.doi.org/10.1594/IEDA/500032>.
- Driscoll, N., Kent, G., and Bormann, J., 2015b, Processed multi-channel seismic data (stacks and migrations) offshore California acquired during the R/V New Horizon expedition NH1320 (2013) using a sparker source: Academic Seismic Portal at UTIG, Marine Geoscience Data System, <http://dx.doi.org/10.1594/IEDA/500041>.
- Fisher, M.A., Normark, W.R., Bohannon, R.G., Sliter, R.W., and A.J. Calvert, 2003, Geology of the continental margin beneath Santa Monica Bay, Southern California, from seismic-reflection data: Bulletin of the Seismological Society of America, v. 93, p. 1955-1983.
- Francis, R., and Legg, M.R., 2010, Quaternary uplift and subsidence of Catalina Ridge and San Pedro basin, Inner California Continental Borderland, offshore southern California; results of high-resolution seismic profiling: Abstract T13C-2218, presented at 2010 Fall Meeting, AGU, San Francisco, California, 13-17 December.
- Grant, L.B., and Rockwell, T.K., 2002, A northward-propagating earthquake sequence in coastal southern California?: Seismological Research Letters, v. 73, no. 4, p. 461–469.
- Junger, A., and H. C. Wagner, 1977, Geology of the Santa Monica and San Pedro Basins, California Continental Borderland, U.S. Geological Survey Map MF-820, scale 1:250,000.
- Hammond, W. C., 2014, Appendix A1 Preliminary GPS Data Evaluation, San Onofre Nuclear Generating Station Seismic Source Characterization SSHAC, Final Project Report: http://www.songscommunity.com/docs/SONGS_2013_SSCSSHAC_PreliminaryModelReportAppendices.pdf (accessed September 2014).
- Henkart, P., 2003, SIOSEIS - a computer system for enhancing and manipulating marine seismic reflection and refraction data: Scripps Institution of Oceanography, University of California San Diego, <http://sioseis.ucsd.edu>.
- Legg, M. R., Goldfinger, G., Kamerling, M.J., Chaytor, J.D., and Einstein, D.E., 2007, Morphology, structure and evolution of California Continental Borderland restraining bends: Geological Society of London Special Publication, v. 290(1), p. 143–168.
- Meade, B.J., and Hager, B.H., 2005, Spatial localization of moment deficits in southern California: Journal of Geophysical Research, v. 110, B04402, doi:10.1029/2004JB003331.
- Normark, W.R., Bohannon, R.G., Sliter, R., Dunhill, G., Scholl, D.W., Laursen, J., Reid, J.A., and Holton, D., 1999a, Cruise report for A1-98-SC Southern California earthquake hazards project: U.S. Geological Survey Open-File Report 99-152, 33 p.
- Normark, W.R., McGann, M., and Sliter, R.W., 2009, Late Quaternary sediment-accumulation rates within the inner basins of the California Continental Borderland in support of geologic hazard evaluation, in Lee, H.J., and Normark, W.R., eds., Earth Science in the Urban Ocean: The Southern California Continental Borderland: Geological Society of America Special Paper 454, p. 117–139, doi: 10.1130/2009.2454(2.6).
- Normark, W.R., Reid, J.A., Sliter, R., Holton, D., Gutmacher, C.E., Fisher, M.A., and Childs, J.R., 1999b,

Cruise report for O1-99-SC Southern California earthquake hazards project: U.S. Geological Survey Open-File Report 99-560, 55 p.

- Paull, C.K., Normark, W.R., Ussler, W., Caress, D.W., and R. Keaten, 2008, Association among active seafloor deformation, mound formation, and gas hydrate growth and accumulation within the seafloor of the Santa Monica Basin, offshore California: *Marine Geology*, v. 250, no. 3-4, p. 258-275, doi: 10.1016/j.margeo.2008.01.011.
- Platt, J.P., and Becker, T.W., 2010, Where is the real transform boundary in California?: *Geochemistry Geophysics Geosystems*, v. 11, no. 6, doi: 10.1029/2010GC003060.
- Plesch, A., et al., 2007, Community Fault Model (CFM) for Southern California: *Bulletin of the Seismological Society of America*, v. 97(6), p. 1793–1802.
- Rockwell, T., 2010, The Rose Canyon Fault Zone in San Diego: *International Conferences on Recent Advances in Geotechnical Earthquake Engineering and Soil Dynamics*, Paper 5.
- Ryan, H.F., Conrad, J.E., Paull, C.K., and McGann, M., 2012, Slip Rate on the San Diego Trough Fault Zone, Inner California Borderland, and the 1986 Oceanside Earthquake Swarm Revisited: *Bulletin of the Seismological Society of America*, v. 102, no. 6, p. 2300–2312, doi: 10.1785/0120110317.
- Singleton, D.M., Rockwell, T.K., Murbach, D., Murbach, M., Maloney, J.M., Freeman, T., and Levy, Y., 2019, Late-Holocene Rupture History of the Rose Canyon Fault in Old Town, San Diego: Implications for Cascading Earthquakes on the Newport–Inglewood–Rose Canyon Fault System: *Bulletin of the Seismological Society of America*, doi: 10.1785/0120180236 (in press).
- Sorlien, C.C., Seeber, L., Broderick, K.G., Luyendyk, B.P., Fisher, M.A., Sliter, R.W., and W. R. Normark, 2013, The Palos Verdes anticlinorium along the Los Angeles, California coast: Implications for underlying thrust faulting: *Geochemistry Geophysics Geosystems*, v. 14, p. 1866–1890, doi:10.1002/ggge.20112.
- Sliter, R.W., Normark, W.R., and Gutmacher, C.E., 2005, Multichannel seismic-reflection data acquired off the coast of Southern California—Part A 1997, 1998, 1999, and 2000: U.S. Geological Survey Open-File Report 2005-1084, <http://pubs.usgs.gov/of/2005/1084/> (accessed April 2014).^[1]
- Triezenberg, P. J., Hart, P. E., and Childs, J. R., 2016, National Archive of Marine Seismic Surveys (NAMSS): A USGS data website of marine seismic reflection data within the U.S. Exclusive Economic Zone (EEZ): U.S. Geological Survey Data Release, <http://dx.doi.org/10.5066/F7930R7P>.
- Wells, D. L., and Coppersmith, K.J., 1994, New empirical relationships among magnitude, rupture length, rupture width, rupture area, and surface displacement: *Bulletin of the Seismological Society of America*, v. 84, p. 974-1002.